

CONFERENCES AND SYMPOSIA

PACS numbers: 01.10.Fv

Scientific session of the Division of General Physics and Astronomy of the Russian Academy of Sciences (22 February 1995)

A scientific session of the Division of General Physics and Astronomy of the Russian Academy of Sciences was held on 22 February 1995 at the P L Kapitza Institute of Physical Problems. The following reports were presented at this session:

(1) **A I Smirnov, I N Khlyustikov** (P L Kapitza Institute of Physical Problems, Moscow) "Magnetoelectric effects and the Stark effect in antiferromagnetic Gd_2CuO_4";

(2) **P E Zil'berman, A G Temiryazev, M P Tikhomirova** (Institute of Radioelectronics, Russian Academy of Sciences) "Short spin waves of exchange nature in ferrite films: excitation, propagation, and potential applications".

Summaries of these papers are given below.

PACS numbers: 75.80.+q; 71.70.Ej; 75.50.Ee

Magnetoelectric effects and the Stark effect in antiferromagnetic Gd_2CuO_4

A I Smirnov, I N Khlyustikov

1. Introduction

The antiferromagnetic Gd_2CuO_4 has an unusual magnetic structure. The copper ion spins become ordered antiferromagnetically at $T_N(Cu) = 280$ K in such a way that the directions of the magnetic moments alternate in a chessboard manner in the basal planes of the tetragonal crystal lattice [1]. The ions of gadolinium become antiferromagnetically ordered at $T_N(Cd) = 6.5$ K. The gadolinium ion spins form ferromagnetic layers magnetised parallel to the basal planes [2] whilst the copper and gadolinium subsystems have different magnetic symmetries. The magnetic structure of the crystal becomes invariant relative to inversion centres, so that the linear magnetoelectric effect can exist. The magnetoelectric effect was discovered in Gd_2CuO_4 [3] because of the appearance of electric polarisation under the influence of a magnetic field (this is known as the ME_H effect). A symmetry analysis of a two-sublattice model of the gadolinium subsystem, carried out in Ref. [3] ignoring the interaction with the copper subsystem, yielded the following terms of the thermodynamic potential responsible for the magnetoelectric effect in the magnetic structure of Gd_2CuO_4:

$$\frac{1}{(4M_0)^2}\,\tilde{\Phi}_{ME} = \lambda M_z(P_xL_x + P_yL_y) + \Lambda P_zML\ . \qquad (1)$$

Uspekhi Fizicheskikh Nauk **165** (10) 1215 – 1224 (1995)
Translated by A Tybulewicz

Here, the x axis is parallel to the [100] direction and the z axis is oriented along the [001] axis of the tetragonal crystal lattice; $2M_0$ is the maximum magnetisation of one of the two gadolinium sublattices; P is the electric polarisation; M and L are, respectively, the magnetisation and the antiferromagnetic vector in units of $4M_0$. A magnetic unit cell contains four gadolinium ions and each of the two sublattices contains (according to this model) two ions.

The magnetic structure of Gd_2CuO_4 is characterised by $L_z = 0$ and two nonzero magnetoelectric moduli α_{zx} and α_{xz}. They are related in the following manner to the magnetoelectric constants λ and Λ:

$$\alpha_{zx} = 4M_0\frac{dM_x}{dE_z} = \frac{dP_z}{dH_x} = 4M_0L\Lambda\chi_{\parallel}k_{zz}\ , \qquad (2)$$

$$\alpha_{xz} = 4M_0\frac{dM_z}{dE_x} = \frac{dP_x}{dH_z} = 4M_0L\Lambda\chi_{\perp}k_{xx}\ . \qquad (3)$$

Here, $\boldsymbol{E}$ and $\boldsymbol{H}$ are the electric and magnetic field intensities; k_{zz} and k_{xx} are the electric susceptibilities: $\chi_{\parallel}$ and $\chi_{\perp}$ are the magnetic susceptibilities along directions parallel and perpendicular to $\boldsymbol{L}$, respectively.

We observed the linear magnetoelectric effect on the basis of the magnetic moment induced by an electric field (ME_E effect), of the linear antiferromagnetic Stark effect, i.e. a shift of the antiferromagnetic resonance (AFMR) spectrum by an electric field, and of the influence of an electric field on the magnetic susceptibility.

These effects can be explained qualitatively within the framework of the two-sublattice model of an antiferromagnetically ordered rare-earth subsystem.

2. Experimental methods

The change in the magnetisation δM under the action of an electric field E was measured with a SQUID magnetometer [4] at 1.2 K. A sample of 1 mm × 1.5 mm × 1 mm dimensions was bonded to flat electrodes by a conducting adhesive. A detection coil revealed the appearance of δM along a direction perpendicular to E.

The microwave magnetic susceptibility χ^{ω} was measured and the AFMR was observed in an electric field with a magnetic resonance spectrometer in a sweep-type cavity without magnetic field modulation. The working frequency of the spectrometer was $f = 35.7$ GHz. An insulated intracavity copper plate created an electric field E perpendicular to an external magnetic field H. A microwave magnetic field h applied to the sample was perpendicular to both H and E.

A small shift of the AFMR line and small changes in χ^{ω} under the influence of an electric field were measured by a modulation method in an alternating electric field of frequency $F = 1.95$ kHz. An alternating component of

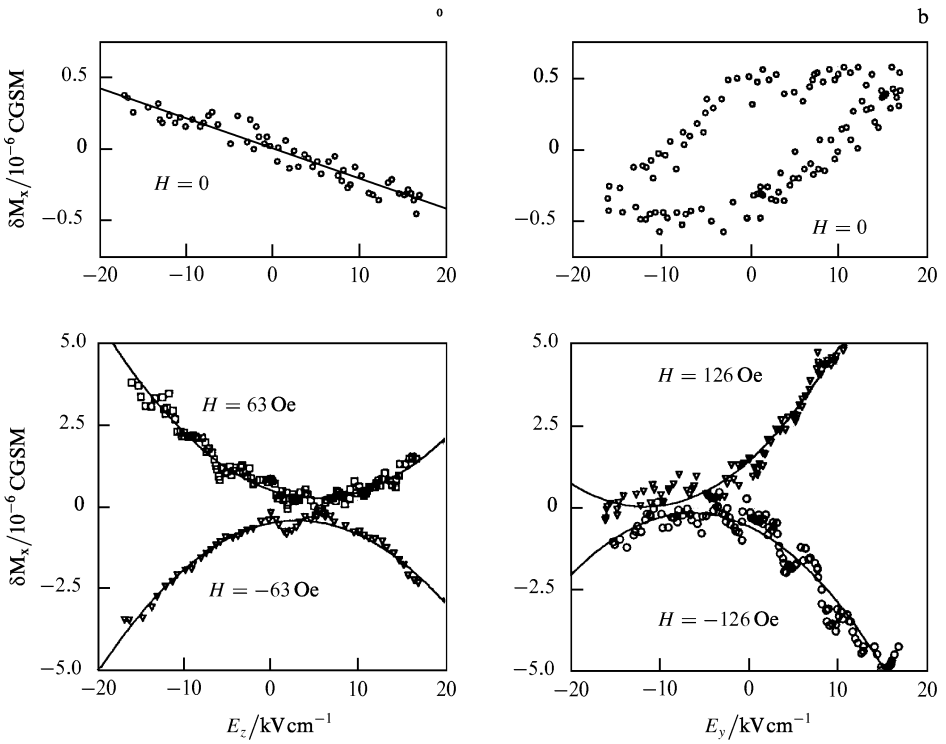

Figure 1. Dependences $\delta M_x(E_z)$ (a) and $\delta M_x(E_y)$ (b) at $T = 1.2$ K.

the microwave power transmitted by the cavity, oscillating at this frequency, appeared as a result of the influence of the field E on χ^{ω}. The amplitude δU of this component was measured with a phase-sensitive amplifier. Should the AFMR magnetic field depend on the applied electric field, then the value of δU should depend on H proportionally to the derivative of the power U of the signal transmitted by the microwave cavity with respect to the magnetic field: dU/dH.

3. Static magnetic properties in an electric field

The static magnetic fields were measured after cooling a sample in zero fields E and H.

The experiments showed that the field E_z produced a linear change δM_x in zero magnetic field (Fig. 1a). This figure shows also the change in the magnetisation as a function of the electric field in an external magnetic field $H_x = 63$ Oe. Such measurements were carried out also in other magnetic fields up to 200 Oe. The results of these experiments were described by the formula $\delta M_x(H) = \alpha E_z + H_x(\beta E_z + \gamma E_z^2)$. Therefore, we detected linear influence of the electric field on the magnetic moment and both linear and quadratic influence on the magnetic susceptibility χ_{xx}.

The electric field E_y altered also the magnetisation M_x and the dependences $\delta M_x(E_y)$ in a zero field had a significant hysteresis (Fig. 1b). This result was evidence of a magnetoelectric coupling between the components M_x and E_y not described by formula (1), and also of the existence of a spontaneous magnetic moment.

4. High-frequency magnetic properties in an electric field

The AFMR in Gd_2CuO_4 had been described in detail and the experimental results were reported in Refs [2, 5]. We studied the influence of the electric field on the lower branch of this resonance, which had a gap of 25.2 GHz at 1.8 K.

The magnetic field was directed in the xz plane at an angle of 45° relative to the x axis and the magnetic field was applied parallel to the y axis. This orientation of the fields made it possible to utilise the interaction of the components M_z and E_y, described by the first term in formula (1), and at the same time to observe the AFMR at the working frequency of the cavity. In the $\boldsymbol{H} \| z$ orientation the AFMR field was too high at this frequency. Fig. 2 shows

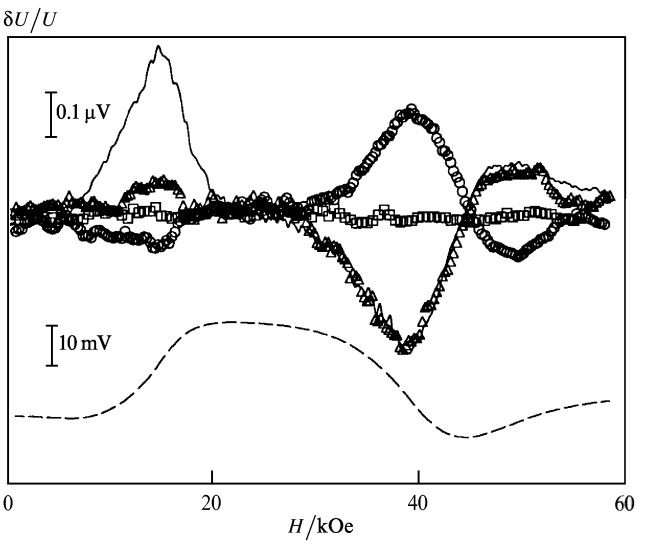

Figure 2. Dependence $\delta U(H)$: (○) after annealing in fields $\boldsymbol{E}$ and $\boldsymbol{H}$; (△) after annealing in the field $\boldsymbol{E}$ reversed; (□) after annealing in zero fields. The continuous curve corresponds to $\alpha = 1.12 \times 10^{-4}$ dU/dH; the dashed curve is the dependence $U(H)$.

the dependences of U, dU/dH, and also of δU on the magnetic field intensity. Near the AFMR line the dependence $\delta U(H)$ was proportional to the derivative dU/dH, indicating a shift of the AFMR field by the electric field.

A single-domain antiferromagnetic state was induced by cooling in fields $\boldsymbol{E}$ and $\boldsymbol{H}$ [6]. The direction of the vector $\boldsymbol{L}$ along the easy axis (which was the bisector of the coordinate angle in the xy plane) was then governed by the sign of the product $\boldsymbol{E}\cdot\boldsymbol{H}$ when going through the Neel temperature. In a sample not subjected to such magnetoelectric annealing the linear magnetoelectric effect was largely compensated by the opposite sign of the effect in the domains that differed in respect of the sign of $\boldsymbol{L}$. Fig. 2 shows the results obtained for a sample cooled in fields $E_y = 3$ kV cm^{-1} and $H = 54$ kOe from 7.5 to 1.2 K, as well as the results obtained after heating to 7.5 K and cooling in the presence of the same field H but with the inverted field $\boldsymbol{E}$. We also included in Fig. 2 the dependence $\delta U(H)$ obtained after cooling in zero fields.

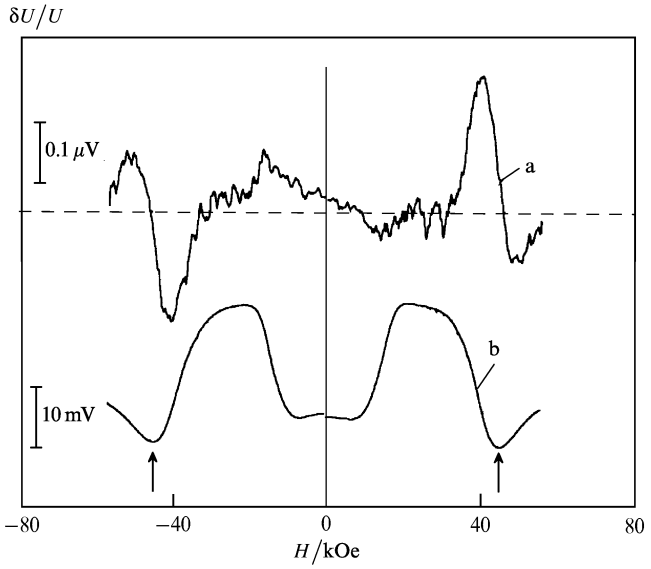

Figure 3. The dependences $\delta U(H)$ for $E = 3$ kV cm^{-1} in the experiment with the inverted magnetic field (a) and $U(H)$ (b); the arrows identify the AFMR fields.

The amplitude δU was used to find the shift δH of the AFMR field, which amounted to 0.1 Oe. It is evident from Fig. 3 that the same electric field increased the absolute value of the AFMR magnetic field in the range of positive magnetic fields and reduced it for an inverted magnetic field. This action of the electric field in our experiments could be due to the appearance of an effective magnetic field directed in the xz plane. The sign of this field changed as a result of reversal of the sign of $\boldsymbol{E}$ or $\boldsymbol{L}$.

It is evident from Figs 2 and 3 that there was a considerable change in the microwave signal U due to a change in H in the range $|H| < 20$ kOe. This was due to a change in the magnetic susceptibility χ_{xx} in the course of spin reorientation in fields $0 < H_x < 9$ kOe [5]. A change in the magnetic susceptibility detuned the cavity and altered the transmitted signal. The value of δU was also significant in these fields (Fig. 2), which indicated the influence of the electric field on the susceptibility χ^{ω} measured relative to the weak field h.

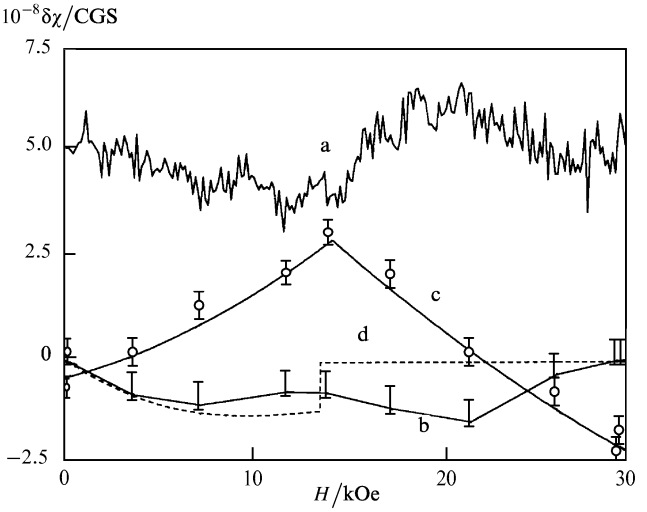

Figure 4. Magnetic-field dependences of: (a) δU; (b) $\delta\chi'$; (c) $\delta\chi''$; (d) dependence $\delta\chi(H)$ calculated in accordance with formula (5).

The dependences of the real and imaginary parts of the change in the susceptibility under the action of the electric field, $\delta\chi'$ and $\delta\chi''$, on the magnetic field are plotted in Fig. 4.

Experiments showed that in the fields below 20 kOe the response δU to the electric field included a considerable contribution with the sign which was reversed when the magnetic field was reversed. This revealed the odd, in terms of $\boldsymbol{E}\cdot\boldsymbol{H}$, correction to the magnetic susceptibility.

We did not detect a linear shift of the AFMR by the electric field in fields $H = H_x$, $E = E_y$, and $H = H_x$, $E = E_z$, but we did observe an influence of the electric field on the susceptibility.

5. Calculations

A description of the antiferromagnetic resonance and of the magnetic susceptibility in an electric field will be based on the thermodynamic potential of a two-sublattice antiferromagnet with a uniaxial anisotropy and a tetragonal anisotropy in a plane [2], supplemented by magnetoelectric terms from formula (1) and also by standard terms describing the interaction of the polarisable medium with the applied electric field. This description is simplistic because it ignores the presence of the copper magnetic subsystem and assumes that the four gadolinium sublattices can be replaced with two. However, the model is sufficient to follow the appearance of several magnetoelectric effects.

The behaviour of the magnetic structure at low temperatures in $E = 0$ and its description on the basis of the proposed model can be found in Ref. [2]. In the ground state the antiferromagnetic vector is parallel to the [110] axis in zero magnetic field. In the $\boldsymbol{H} \parallel \boldsymbol{x}$ configuration an increase in the magnetic field from zero to H_c rotates the vector $\boldsymbol{L}$ towards the [010] direction, but a further increase in the field does not alter the orientation of $\boldsymbol{L}$, which remains perpendicular to the magnetic field. Here $H_c = (4H_tH_e)^{1/2}$; H_t is the tetragonal anisotropy field; H_e is the exchange field. When the field reaches $H = H_c$, a second-order phase transition takes place. In view of the large difference between the values of $\chi_{\parallel}$ and $\chi_{\perp}$ and also because of the nonuniform rotation of the magnetisation when the magnetic field is varied, the susceptibility depends on the

magnetic field in the range from zero to H_c, and at the point $H = H_c$ the susceptibility χ_{xx} is abruptly halved. In fields $H > H_c$, the susceptibility does not change any more and it remains equal to $\chi_\perp$.

The Landau–Lifshitz equations of motion, derived on the basis of the potential described above, lead to the following expression for the shift of the AFMR field at frequency ω when $H_z = H_x = H/\sqrt{2}$, $H_x > H_c$, $H_y = 0$:

$$\delta H = \sigma\left(\frac{1}{\sqrt{2}} + 2\,\frac{H_t\left[(\omega/\gamma)^2 - H^2\right]}{H\left[2(\omega/\gamma)^2 + 4H_e H_t - 2H_A H_e\right]}\right). \quad (4)$$

Here, γ is the magnetomechanical ratio and $\sigma = 4M_0\lambda P_y L_y$. The quantity σ is the effective magnetic field with its sign reversed:

$$H_{\text{eff}} = -\frac{1}{4M_0}\,\frac{\mathrm{d}\tilde{\Phi}_{\text{ME}}}{\mathrm{d}M},$$

which appears along the z axis under the action of the electric field E_y, and H_A is the uniaxial anisotropy field.

The second term in the formula for the shift represents 0.14 of the first term. The electric field therefore alters the z projection of the AFMR field by an amount practically equal to the effective field σ.

A similar calculation shows that the linear AFMR shift produced by the electric field is also absent for $\boldsymbol{E} \| z$, $\boldsymbol{H} \| x$. This circumstance can be explained by the fact that the effective field is now perpendicular to the external magnetic field and that the change in the combined magnetic field is a quadratic function of $\boldsymbol{E}$.

Minimisation of the potential under the conditions $\boldsymbol{L} \perp \boldsymbol{M}$, where $L^2 + M^2 = 1$, typical of low temperatures, gives the following expression of the change in the magnetic susceptibility under the influence of the electric field when $H_x = H_z$, $H_x < H_c$:

$$\delta\chi_{xx} = -\chi_\perp\,\frac{4M_0\lambda P_y}{H_c}\,\frac{H}{H_c}\,\frac{1}{\left[1 + (H/\sqrt{2}H_c)^2\right]^{3/2}}. \quad (5)$$

The physical meaning of this result is that in the presence of a nonzero magnetic field along the z axis the electric field alters the orientation of the vector $\boldsymbol{L}$ relative to the magnetic field and this changes the magnetic susceptibility.

6. Discussion

The observed AFMR shift by the electric field is in agreement with the value of the magnetoelectric modulus α_{xz} [3] and of the susceptibility $\chi_\perp$, in accordance with formula (4).

We shall now use the characteristics of the magnetoelectric effect determined for Gd_2CuO_4 to estimate the influence of the electric field on the susceptibility, in accordance with the calculations given above.

If $E = E_y$, $H_x = H_z$, the AFMR shift means that the quantity $4M_0\lambda P_y$ has the value 0.15 Oe in the field $E_y = 3\ \text{kV cm}^{-1}$. Then, formula (5) gives the dependence $\delta\chi_{xx}(H)$ plotted in Fig. 4 (line d). We determined the dynamic susceptibility at a frequency of the order of the AFMR frequency; its value could differ considerably from the static susceptibility. In this experiment the results could be influenced not only by the susceptibility χ^{ω}_{xx}, but also by χ^{ω}_{zz}. Formula (5) is derived with account taken of the change in the static susceptibility χ_{xx}. In view of these circumstances, the agreement between the orders of magnitude and the nature of the dependence on the magnetic field found for the observed quantities $\delta\chi'$ and $\delta\chi''$ and the calculated quantity $\delta\chi_{xx}(H)$ seems to be satisfactory.

It therefore follows that the changes in the magnetic susceptibility, which are odd in EH (Figs 2 and 3), can be explained on the basis of a simplified model of the effect: if $H \neq 0$, the electric field alters the orientation of the vector $\boldsymbol{L}$ and changes the susceptibility.

The linear AFMR shift at $H_z = H_x$ and its absence at $\boldsymbol{H} \| \boldsymbol{x}$ are also in good agreement with our calculation of the AFMR shift in the electric field.

However, the adopted model cannot account for the magnetic moment δM_x induced by the electric field E_y, for the weak ferromagnetic moment, and for the electric-field-dependent magnetic susceptibility in zero magnetic field. Moreover, the weak ferromagnetism, due to the terms bilinear in L and M, is forbidden for tetragonal crystals. However, a weak ferromagnetic moment has been observed [7] at temperatures below T_N(Cu) and above T_N(Gd). This moment has been explained on the assumption that the tetragonal lattice is slightly distorted [8]. We observed a spontaneous moment of at least $\sim 10^{-9} M_0$ at temperatures below T_N(Gd) (Fig. 1b). The magnetoelectric interaction, corresponding to a term of the potential proportional to $E_x M_y$ observed in our experiments (Fig. 2b), is also impossible for the initial crystallographic group $I4mmm$. Obviously, the spontaneous magnetic moment generates, by the magnetoelectric interaction, also a spontaneous electric polarisation. In this case the antiferromagnet Gd_2CuO_4 behaves similarly to nickel iodine boracite [9], which is a weakly ferromagnetic magnetoelectric ferroelectric.

The components of the magnetic field linear in $\boldsymbol{E}$, observed in zero magnetic field for $\boldsymbol{E} \| \boldsymbol{y}$ and $\boldsymbol{E} \| \boldsymbol{z}$, can be attributed to the presence of $pE_i M_j^2 L_k^2$ type terms in the expansion of the thermodynamic potential. The component of the magnetic susceptibility quadratic in the electric field (Fig. 1) can be described by introducing also terms of the $qE_i^2 M_j^2 L_k^2$ type. However, the observed effects can be explained by analogy with Section 5, by inclusion of lower-order terms which are of the $L_y M_x \pm L_x M_y$, $E_y M_x L_y$, $E_y M_y L_z$ type and are due to distortions of the original struture.

We shall conclude by listing the terms of the thermodynamic potential Φ in terms of the variables E and H, which should be included in this potential in order to describe the magnetoelectric effects observed by us:

$$\Phi_{\text{ME}} = k_i H_i + \alpha_{ik} E_i H_k + \gamma_{ik} E_i H_k^2 + \beta_{ikl} E_i H_k H_l^2 + \tau_{ik} E_i^2 H_k^2. \quad (6)$$

Our experiments revealed that there are nonzero coefficients α_{zx}, α_{xy}, α_{xz}, γ_{zx}, γ_{xz}, β_{xzx}, β_{zxy}, τ_{zx}, τ_{xy}, τ_{xz}, k_x.

Acknowledgement. This work was supported by the International Science Foundation and by the Russian Fund for Fundamental Research.

References

1. Chattopadhyay T, Brown P J, Roessli B, et al. *Phys. Rev. B* **46** 5731 (1992)
2. Chattopadhyay T, Brown P J, Stepanov A A, et al. *Phys. Rev. B* **44** 9486 (1991)

3. Wiegelmann I, Stepanov A A, Vitebsky I M, et al. *Phys. Rev. B* **49** 10039 (1994)
4. Khlyustikov I N *Prib. Tekh. Eksp.* (2) 167 (1993)
5. Zvyagin A I, Yablonskii D A, Pashchenko V A, et al. *Fiz. Nizk. Temp.* **18** 12 (1992) [*Sov. J. Low Temp. Phys.* **18** 6 (1992)]
6. Astrov D N *Zh. Eksp. Teor. Fiz.* **38** 984 (1960) [*Sov. Phys. JETP* **11** 708 (1960)]
7. Thompson J D, Cheong S-W, Brown S E, et al. *Phys. Rev. B* **39** 6660 (1989)
8. Stepanov A A, Wyder P, Chattopadhyay T, et al. *Phys. Rev. B* **48** 12979 (1993)
9. Ascher E, Rieder H, Schmid H, Stossel H *J. Appl. Phys.* **37** 1404 (1966)

PACS numbers: 75.30.Ds; 75.30.Et; 75.50.Gg

Short spin waves of exchange nature in ferrite films: excitation, propagation, and potential applications

P E Zil'berman, A G Temiryazev, M P Tikhomirova

1. Introduction

There are two mechanisms of energy transfer in a spin wave: (1) the magnetic-dipole interaction of the spins: (2) the exchange interaction. The first of these mechanisms predominates in what are known as magnetostatic waves. The waves in which the second mechanism predominates will be called exchange spin waves.

The exchange spin waves (ESWs) were discovered in the famous work of Bloch on the subject [1]. They can have very short wavelengths, $\lambda < 1$ μm, and therefore they occupy the main part of the phase space of elementary excitations in a ferrite. Very few experimental investigations have been made so far of ESWs. Much more work has been done on long-wavelength ($\lambda > 20$ μm) magnetostatic spin waves. Suffice to say that up to now there have been no effective methods for the excitation of ESWs with a given frequency and direction of propagation. We would like to report here the main ideas and results of our recent investigations designed to master travelling ESWs as a new experimental method and means for signal processing.

2. Electromagnetic excitation of exchange spin waves

The problem is how to achieve phase-matched excitation in spite of a large difference between the wavelength of the exciting electromagnetic wave (λ_{EM}) and the wavelength of the excited ESW (λ). For example, typical orders of magnitude are: $\lambda_{EM} \sim 1-10$ cm and $\lambda \sim 0.1-1$ μm. The required phase matching can be ensured by converters (antennas). A converter can, in principle, be an electrodynamic inhomogeneity near the surface or in the interior of a ferrite created in any way. It is important that the spectrum of spatial harmonics of the electromagnetic field around such an inhomogeneity should include a harmonic with a wave vector $\boldsymbol{q}$. Then, if the spectrum of a ferrite includes an ESW with a wave vector $\boldsymbol{q}$ at the frequency of the electromagnetic wave, then this ESW can be excited.

Fig. 1 shows schematically how spin waves can be excited by a metal strip carrying a microwave current, which is brought close to a ferrite film. A magnetic field $\boldsymbol{h}$ of the microwave current $\boldsymbol{j}$ varies over distances of the order of the strip width w. Therefore, this magnetic field should be capable of exciting spin waves with $q \leqslant \pi/w$. For typical values $w \sim 20-50$ μm this gives $\lambda = 2\pi/q \geqslant 40-100$ μm. Further considerable reduction in the wavelength by reducing w meets with considerable difficulties because such very narrow strips cannot be matched to the existing microwave current sources.

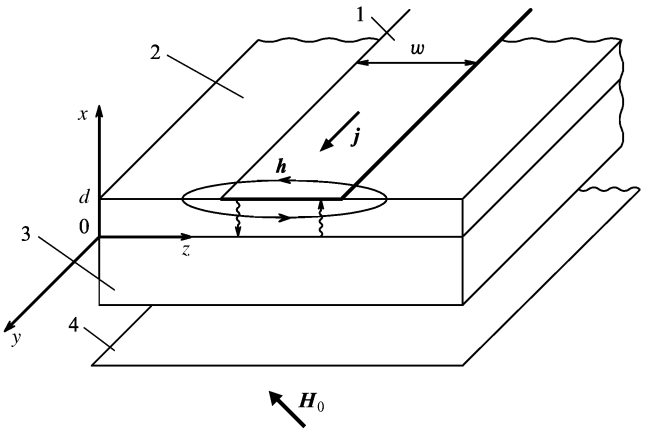

Figure 1. Structure for the excitation of exchange spin waves: (*1*) metal strip of width w; (*2*) ferrite film of thickness d; (*3*) substrate; (*4*) earthed metal base; (*5*) $\boldsymbol{H}_0$ is a static external magnetic field; (*6*) $\boldsymbol{h}$ is a microwave magnetic field of the current $\boldsymbol{j}$ (identified by an arrow); a closed curve with arrows is a line of force of $\boldsymbol{h}$; wavy lines represent the excited and reflected exchange spin waves.

However, there is a simple way of exciting short ESWs associated with the presence of the boundary surface of a film. Such a surface creates an inhomogeneity along the direction of its normal. Therefore, the excited ESWs should travel along the normal. Let us consider this for a surface with totally pinned spins. Let us assume that for $x = d$ (Fig. 1) the angle of precession of the magnetisation in a field $\boldsymbol{h}$ is zero (pinned spins). Then, near the surface, at distances of the order of the exchange length $l_{exch} \sim 10^{-6}$ cm from the surface, this angle gradually increases from zero to its normal value in the interior of the ferrite film. The inhomogeneity of the angle of precession in the surface layer plays the role of an antenna capable of emitting short ESWs with $\lambda \geqslant l_{exch}$.

It would seem that this mechanism for the excitation of ESWs would have been deduced a long time ago from spin-wave resonance experiments [2]. However, in the spin-wave resonance a wave is reflected from the opposite surface $x = 0$ and, on return to the initial surface $x = d$, it transforms back into a microwave signal. The resonance is observed only when there is sufficient accumulation of energy in a plane-parallel ferrite cavity after many trips of the wave between the surfaces $x = 0$ and $x = d$. Therefore, observation of this resonance cannot by itself provide information on the efficiency of the conversion process.

The first experimental investigation of the excitation of short ESWs under propagation conditions was reported in Ref. [3]. Rectangular microwave current pulses were generated in a strip converter (Fig. 1) and the excitation of ESWs was detected on the basis of echo pulses, representing the results of back conversion of spin waves that returned to the converter after reflection from the opposite boundary of the film. The duration of the ESW pulse was less than its

travel time across the film thickness. Therefore, energy accumulation did not occur in the film. It was found that without a special treatment of the film surface it was not possible to observe any echo pulses even if clear spin-wave resonance lines were observed under continuous excitation conditions. The echo pulses appeared only when He and Ne ions were implanted in the films. The conversion efficiency estimated from the intensity of these echo pulses was then fairly high (of the order of 30%).

What was the role of the implantation process? The assumption that implantation enhanced surface pinning of spins was used in Ref. [4] to calculate the efficiency of excitation of ESWs. The film was assumed to be homogeneous but the boundary condition of spin pinning was imposed on the $x = 0$ surface. A calculation was made of the ESW energy flux carried away from a strip into the film. Without going into details, it was found that under realistic conditions the efficiency of excitation is low (of the order of 0.03%) for any degree of spin pinning. This estimate would explain why the echo pulses were not observed in the experiments on unimplanted homogeneous films, but the role of implantation is not clear. In this case, the role of implantation does not reduce simply to enhancement of spin pinning. Further experiments [5] have provided more information on this topic.

3. Experiments on exchange spin waves in YIG films with variable thickness

The experimental setup is shown in Fig. 2. A film (*1*) was pressed by means of an insulating spacer (500 – 100 μm thick) against a metal strip (*2*) which was $w = 0.5$ mm wide. A microwave power P_{in} was coupled into the strip via a circulator (*3*). The reflected power P_{out} was also coupled out through the circulator and investigated as a function of an external field $\boldsymbol{H}_0$ at a fixed frequency ω or as a function of the frequency ω when the field $\boldsymbol{H}_0$ was fixed. The investigated films were $d = 10 - 20$ μm thick and their dimensions in their own plane were several centimetres. Among these films there were some with an anomalously wide (hundreds of megahertz) absorption spectrum.

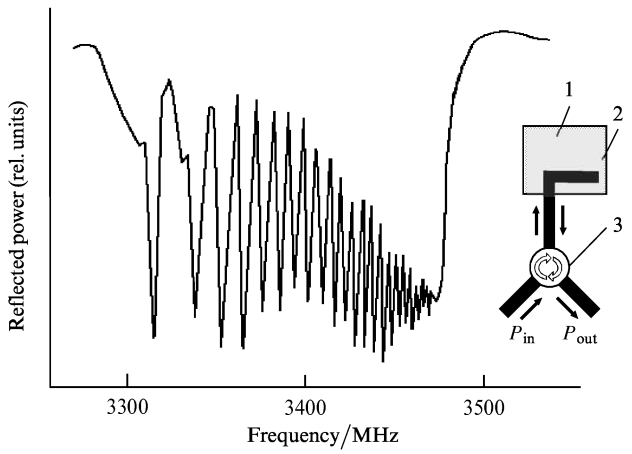

Figure 2. Wide absorption spectrum showing the frequency dependence of the microwave power reflected from a sample (a YIG film with the [111] orientation magnetised in a field $\boldsymbol{H}_0$ parallel to the surface; $d = 12.5$ μm; $H_0 = 564$ Oe) and the experimental setup used in the measurements: (*1*) YIG film; (*2*) strip converter; (*3*) circulator; P_{in} is the incident microwave power; P_{out} is the reflected microwave power.

Fig. 2 shows a typical absorption spectrum of such a film. Inside a wide dip of P_{out} plotted against frequency there were reflection peaks. Variation of the dimensions of the film in its own plane had no influence on these peaks. Hence, we concluded that the peaks appeared because of a spin-wave resonance across the thickness. The frequencies ω_n of the spin-wave resonance peaks of a homogeneous film should depend on the resonance number n as n^2 [2]. Any deviations from this law would indicate an inhomogeneity of the magnetic parameters of a film [6, 7]. In our case (Fig. 2), the n^2 law was not obeyed. Experiments show that, although the actual dependence of ω_n on n differed from film to film or as a result of variation of the direction of the field $\boldsymbol{H}$, the n^2 law was not obeyed by all the films with an anomalously wide absorption spectrum.

Fig. 3 gives typical dependences of the frequencies ω_n at the centre of a peak on the number n plotted on the basis of the measured absorption spectra. When the field $\boldsymbol{H}$ was parallel to the surface, tens of peaks were observed and the density of the peaks increased with n. When the field $\boldsymbol{H}$ was perpendicular to the surface, the number of peaks increased to 120 (for the same film) and all of them were equidistant. The width of the absorption spectrum was then about 1 GHz.

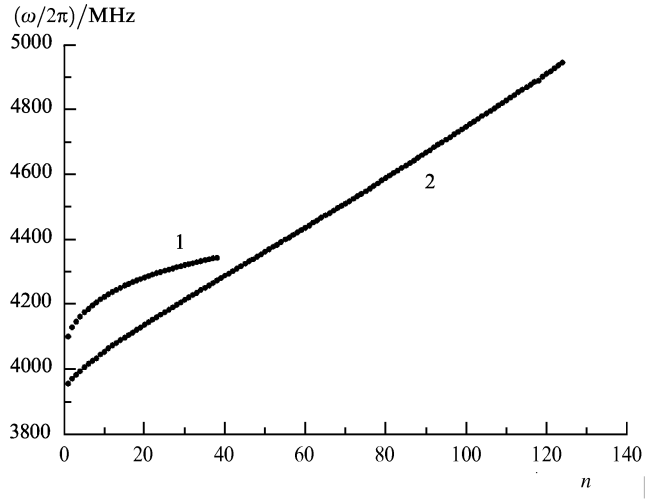

Figure 3. Dependence of the resonance frequency ω_n on the resonance number n: (*1*) YIG film [111] orientation ($d = 17$ μm} in a parallel magnetic field $H_0 = 808$ Oe; (*2*) same YIG film in a perpendicular field $H_0 = 3505$ Oe.

The deviations from the n^2 law were indeed due to the inhomogeneity of our films. A technology for the growth of YIG films by the method of liquid-phase epitaxy with a specified inhomogeneity profile had been developed by A V Maryakhin and A S Khe. Our own investigations of such films showed unambiguously that the spin-wave resonance spectrum could be synthesised as desired by a suitable selection of the inhomogeneity profile.

It is worth noting the considerable depth of the dip of P_{out} at frequencies outside the resonance peaks. At such frequencies there was practically no reflection of the microwave signal. This absence of reflection provides evidence of the high efficiency of the excitation of ESWs.

4. Theoretical description of exchange spin waves in inhomogeneous films

The theory presented below is based on the observation that the exchange length (l_{exch}) is considerably less than the inhomogeneity scale (Λ):

$$l_{\text{exch}} \ll \Lambda . \tag{1}$$

In fact, Λ is determined either by the film thickness or by the thickness of the implanted layer, i.e. it lies within the range 10–1 μm, which is 2–3 orders of magnitude greater than l_{exch}.

The wavelength $\lambda(x)$ of ESWs varies in the course of propagation in an inhomogeneous film. At those points inside the film where the conditions $l_{\text{exch}} \leqslant \lambda(x) \ll \Lambda$ are satisfied, the propagation can be described in the WKB approximation. However, these conditions may not be obeyed near some points l, called the 'turning points', at which $\lambda(l) \to \infty$. The exact solution can be obtained near such turning points and then fitted to the WKB solution. As a result, the excitation of ESWs occurs specifically near the turning points, where λ is large and the best matching to an electromagnetic wave is achieved.

From now on, we shall consider only the films with a monotonic inhomogeneity profile. Inside such films there is only one turning point and the coordinate of this point l depends on ω and H_0. It is convenient to introduce the change in the ESW phase:

$$\varphi(\omega, H_0) = 2\int_0^{l(\omega, H_0)} |q(x, \omega, H_0)|\,\mathrm{d}x + \varphi_0 , \tag{2}$$

where $0 \leqslant l(\omega, H_0) \leqslant d$. The first term describes the phase shift as a result of propagation and the second is the phase jump on reflection of an ESW from the $x = 0$ surface ($\varphi_0 = 3\pi/2$ for free spins and $\varphi_0 = \pi/2$ for pinned spins). The expression for the exchange spin wave number q depends on the direction of $\boldsymbol{H}_0$. If $\boldsymbol{H}_0$ is perpendicular to the film, this expression is

$$q(x)^2 = \frac{1}{D}\left[\frac{\omega}{\gamma} - H_0 + 4\pi M(x)\right], \tag{3}$$

where D is the exchange constant; γ is the gyromagnetic ratio; $4\pi M(x) = 4\pi M_{\text{S}}(x) - H_{\text{A}}(x)$, M_{S} is the saturation magnetisation; $H_{\text{A}}(x)$ is the anisotropy field. In terms of the phase defined by Eqn (2), the condition for a spin-wave resonance can be formulated quite simply:

$$\varphi(\omega_n, H_0) = 2\pi n \tag{4}$$

for each $n = 1, 2, \ldots, N$.

Eqns (2)–(4) describe well the experimental results. In particular, these equations make it possible to reconstruct the inhomogeneity profile $[4\pi M(x)]$ from the experimentally determined spin-wave resonance frequency ω_n. The assumption that $q^2 = 0$ makes it possible to find from expression (3) a sequence of values of $4\pi M_n$ at the turning points where the frequencies are $\omega = \omega_n$. The profile can now be reconstructed simply by finding the coordinates of all the turning points $l(\omega_n, H_0)$. Let us approximate the dependence $4\pi M(x)$ between consecutive turning points by a linear function and let us substitute it into the system of equations (4), bearing in mind the definition given by Eqn (2). Then, the system of equations (4) yields all the coordinates $l(\omega_n, H_0)$. A typical profile reconstructed in this way is shown in Fig. 4. We can see that practically the same

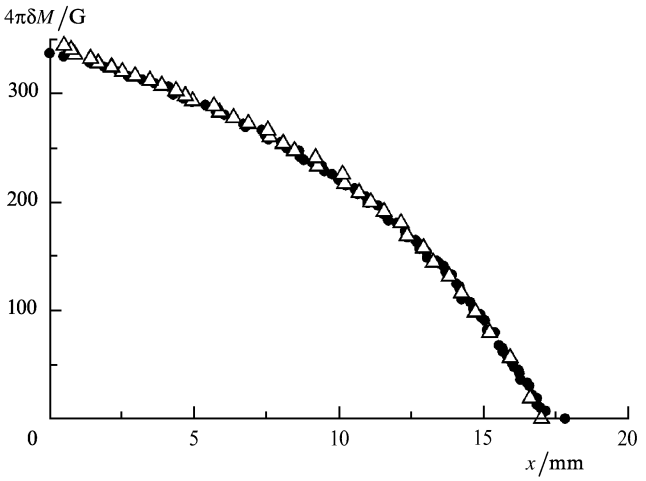

Figure 4. Reconstructed profile of the relative change in the effective magnetisation $4\pi\delta M(x) \equiv 4\pi M(x) - 4\pi M(d)$ across the thickness of a YIG film with the [111] orientation; $d = 17$ μm. The results were obtained by an analysis of the spectra shown in Fig. 3: (●) data calculated from the spectra of a perpendicularly magnetised film; (△) data deduced from the spectra of a film magnetised parallel to its surface.

profile is obtained irrespective of the direction of $\boldsymbol{H}_0$. This confirms the correctness of the adopted theoretical model.

In this model the limits of the absorption bands are determined by those frequencies ω_0 and ω_d at which the turning point first enters the film and then leaves it. According to Eqn (3), these frequencies are $\omega_0 = \gamma(H_0 - 4\pi M_0)$ and $\omega_d = \gamma(H_0 - 4\pi M_d)$. Then the width of the absorption band is $\Delta\omega = |\omega_0 - \omega_d| = 4\pi\gamma|M_0 - M_d|$, where $M_0 = M(0)$ and $M_d = M(d)$. Substitution of the difference $|M_0 - M_d|$, deduced from the reconstructed profile (Fig. 4), gives an estimate which is in agreement with the experimental results.

Let us assume that $M(x)$ can be represented by the power law $4\pi M(x) = 4\pi M_0 - 4\pi(M_0 - M_d)(x/d)^r$. Substitution of this law into Eqns (3) and (2) gives

$$\varphi(\omega) = C(\omega - \omega_0)^{(r+2)/2r}, \quad \omega_0 \leqslant \omega \leqslant \omega_d , \tag{5}$$

where the coefficient C is independent of ω. According to expression (5), the frequency dependence of the phase and, therefore, the line positions in the spin-wave resonance spectrum are governed by the power exponent r. In particular, if $r = 2$, the phase increases linearly with the frequency. Precisely this type of dependence is found experimentally (Fig. 3) for films with a parabolic profile in a field normal to the film plane. Expression (5) also suggests an interesting possibility of synthesis of the frequency dependence $\varphi(\omega)$ by selection of a suitable profile (exponent r).

5. Propagation of exchange spin-wave pulses in inhomogeneous films

As pointed out earlier, an estimate of the efficiency of the excitation of travelling ESWs can be obtained in experiments under pulsed conditions, with no changes in the experimental setup shown in Fig. 2. Fig. 5 reproduces oscillograms of the reflected pulses of P_{out} obtained for different fields H_0 and two orientations of the field. The film had a parabolic inhomogeneity profile with a power exponent $r = 2$. In the absence of the field ($H_0 = 0$) a pulse

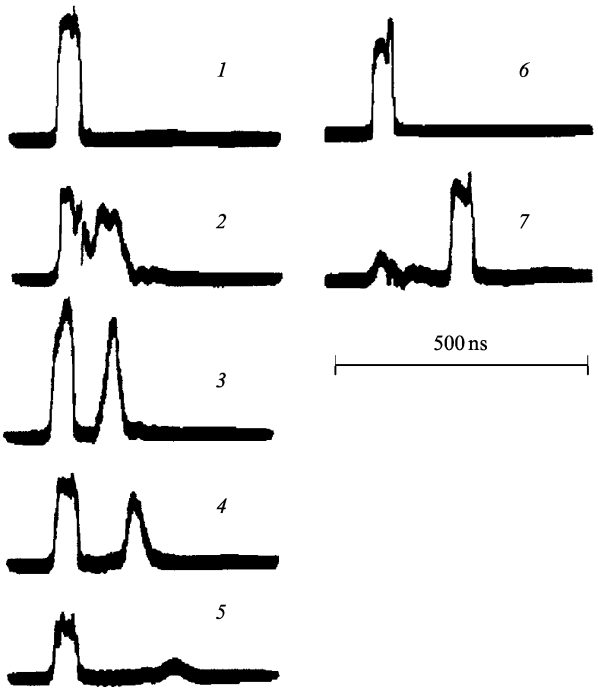

Figure 5. Time dependence of the envelope of the reflected signal. (*1–5*) Parallel field, $\omega/2\pi = 5124$ MHz; (*1*) $H_0 = 0$, $K = 0$; (*2*) $H_0 = 1084$ Oe, $K = 10$ dB; (*3*) $H_0 = 1079$ Oe, $K = 10$ dB; (*4*) $H_0 = 1071$ Oe, $K = 10$ dB; (*5*) $H_0 = 1058$ Oe, $K = 10$ dB. (*6, 7*) Normal field, $\omega/2\pi = 5322$ MHz: (*6*) $H_0 = 0$, $K = 0$; (*7*) $H_0 = 3790$ Oe, $K = 7.6$ dB (YIG film, [111] orientation, $d = 15$ μm).

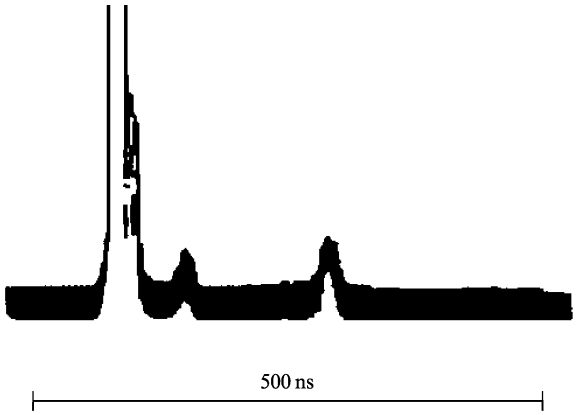

Figure 6. Time dependence of the envelope of the reflected signal (normal field $H_0 = 2933$ Oe, $\omega/2\pi = 3695$ MHz, YIG film [111] orientation, $d = 15$ μm).

of P_{in} was reflected totally. As H_0 was increased, a second delayed pulse of P_{out} appeared in a certain range of the field. When the field H_0 was parallel to the film plane, the delay time τ depended strongly on H_0 and for the normal orientation the value of τ was practically independent of H_0.

We can estimate τ, subject to expression (5), as follows:

$$\tau(\omega) \equiv \frac{\partial\varphi}{\partial\omega} = C\,\frac{r+2}{2r}(\omega-\omega_0)^{(2-r)/2r}. \qquad (6)$$

According to expression (6), if $r = 2$, the frequency dependence of τ disappears, i.e. the delay becomes dispersion-free. This conclusion is in agreement with the pattern of pulses shown in Fig. 5 (*6* and *7* demonstrate that a delayed pulse suffers practically no dispersion distortion of its profile).

The pulses in Fig. 5 correspond to different values of the input power P_{in}. The values of K, given in the figure caption, demonstrate the relative change in this power. A comparison of the pulses can be used to estimate the relationship between P_{out} and P_{in}. We can therefore conclude that the total losses due to the excitation, propagation, and reception of ESWs are relatively small and are of the order of 10 dB for delay times $\tau = 100-140$ ns.

6. Interaction of exchange spin waves with ultrasound in inhomogeneous films

This interaction has been observed earlier in experiments on YIG rods [8], when an inhomogeneity was observed because of demagnetisation fields. In our experiments the interaction of ESWs with ultrasound was observed in YIG films with an inhomogeneity of the anisotropy field across the thickness. At some point l_s inside the film ($0 < l_s < l \leqslant d$) the following phase-matching condition may be satisfied:

$$\lambda(l_s) = \lambda_s, \qquad (7)$$

where λ_s is the wavelength of ultrasound. This results in the excitation of an ultrasonic wave and its propagation alongside an ESW.

Fig. 6 reproduces an oscillogram of P_{out} showing two delayed pulses. The pulse with the largest delay may be associated with the propagation of ESWs. The less delayed pulse propagates as an ultrasonic wave in the section $0 \leqslant x \leqslant l_s$. We can see that the intensities of both pulses are comparable, i.e. that ultrasound is excited as efficiently as ESWs. The maximum frequency of the excited ultrasound is determined by the magnetisation 'drop' $\Delta M = |M_0 - M_d|$, namely [5]

$$\omega_{max} = V_s\left(\frac{4\pi\Delta M}{D}\right)^{1/2}, \qquad (8)$$

where V_s is the velocity of sound. Estimates show that it was possible to excite ultrasound at frequencies 16–20 GHz in our films with $4\pi\Delta M \sim 300-500$ G. We detected experimentally the excitation at frequencies up to 18 GHz.

7. Potential applications

Pulses or parallel beams of short ESWs make it possible to probe magnetic films so as to obtain information about their local properties. For example, the possibility of spin-wave location of domain walls in ferromagnets is considered in Ref. [9]. This application of short ESWs provides essentially a new experimental method, which supplements the widely used spin-wave resonance method. By analogy with the familiar acoustic microscope method, the new method can be called the 'spin-wave microscope', although naturally it is still at the early stage of development.

Short ESWs may be used as a new information carrier in electronic signal-processing devices. Ultrasonic and magnetostatic waves have been used so far for this purpose. However, the devices based on ultrasonic waves cannot be frequency-tuned over a wide range and those based on

magnetostatic waves are fairly large and heavy. The advantages of devices based on ESWs could be: (1) a reduction in the dimensions, principally possible because of the short wavelengths ($\lambda < 1$ μm): (2) frequency tuning and control of the characteristics; (3) feasibility of synthesis of the required characteristics; (4) new functional possibilities associated with the specifics of the exchange interaction.

Finally, ESWs may be used for the efficient excitation of ultrasonic waves of very high frequencies (up to 20 GHz or higher). Such excitation occurs in a wide ($\sim$1 GHz) frequency band. The excitation efficiency is high: of the order of 30%.

Acknowledgements. This work was partly supported by the International Science Foundation (ISF Grant No. MSZ000) and by the Russian Fund for Fundamental Research (Grant No. 94-02-04928-a).

References

1. Bloch F *Z. Phys.* **61** 206 (1930)
2. Wigen P E *Thin Solid Films* **114** 135 (1984)
3. Gulyaev Yu V, Zil'berman P E, Sannikov E S, Tikhonov V V, Tolkachev A V *Pis'ma Zh. Tekh. Fiz.* **14** 884 (1988) [*Sov. Tech. Phys. Lett.* **14** 391 (1988)
4. Zil'berman P E, Shishkin V G *Radiotekh. Elektron.* **35** 204 (1990)
5. Zil'berman P E, Temiryazev A G, Tikhomirova M P *Zh. Eksp. Teor. Fiz.* (in press)
6. Portis A M *Appl. Phys. Lett.* **2** 69 (1963)
7. Schlomann E *J. Appl. Phys.* **36** 1193 (1965)
8. Schlomann E, Joseph R I *J. Appl. Phys.* **35** 2382 (1964); Erratum: *J. Appl. Phys.* **36** 875 (1965)
9. Zil'berman P E, Umanskii A V *Zh. Tekh. Fiz.* **58** 1572 (1988) [*Sov. Phys. Tech. Phys.* **33** 946 (1988)]